



## OPEN ACCESS

## EDITED BY

Mario G. S. Ferreira,  
University of Aveiro, Portugal

## REVIEWED BY

Khaled Jawad Habib,  
Kuwait Institute for Scientific Research,  
Kuwait  
Mehmet Fatih Kaya,  
Erciyes University, Turkey

## \*CORRESPONDENCE

Helene Conseil-Gudla,  
helco@dtu.dk

## SPECIALTY SECTION

This article was submitted to  
Environmental Degradation of Materials,  
a section of the journal  
Frontiers in Materials

RECEIVED 22 July 2022

ACCEPTED 21 October 2022

PUBLISHED 02 November 2022

## CITATION

Rao JM, Yadav A, Conseil-Gudla H and  
Ambat R (2022), Synergetic effect of  
temperature and humidity on the  
leakage of KOH electrolyte and related  
reliability of zinc-air batteries.  
*Front. Mater.* 9:1000808.  
doi: 10.3389/fmats.2022.1000808

## COPYRIGHT

© 2022 Rao, Yadav, Conseil-Gudla and  
Ambat. This is an open-access article  
distributed under the terms of the  
[Creative Commons Attribution License  
\(CC BY\)](https://creativecommons.org/licenses/by/4.0/). The use, distribution or  
reproduction in other forums is  
permitted, provided the original  
author(s) and the copyright owner(s) are  
credited and that the original  
publication in this journal is cited, in  
accordance with accepted academic  
practice. No use, distribution or  
reproduction is permitted which does  
not comply with these terms.

# Synergetic effect of temperature and humidity on the leakage of KOH electrolyte and related reliability of zinc-air batteries

Jyothsna Murli Rao<sup>1</sup>, Abhijeet Yadav<sup>2</sup>, Helene Conseil-Gudla<sup>1\*</sup>  
and Rajan Ambat<sup>1</sup>

<sup>1</sup>Department of Civil and Mechanical Engineering, Technical University of Denmark, Lyngby, Denmark, <sup>2</sup>R&D Department, WS Audiology, Lynge, Denmark

The Zinc-air primary batteries (ZAB's) are prone to electrolyte leakage upon exposure to high temperature and humidity conditions. Potassium hydroxide is a hygroscopic and corrosive compound and it can cause various electrochemical corrosion failures for the attached electronics inside a device. In this study, the effect of temperature and humid conditions on the leakage of Potassium hydroxide electrolyte from three different Zinc Air Battery variants were investigated. The batteries were exposed to hot and humid conditions, and a qualitative Gel test with pH indicator was used to visually observe the leakage from the individual set of battery variants. The residues of the released electrolyte was identified by FTIR and quantified using a titration method. SEM-EDS analysis was also performed to examine the surface of the batteries and sealants for eventual damage. The related effect of electrolyte leakage on the reliability of the batteries was performed by a voltage discharge test. The hygroscopicity properties of pure Potassium hydroxide were studied using a water sorption/desorption equipment and was correlated with electro impedance spectroscopy analysis using an interdigitated test board. The results from the study indicate that the increase in temperature caused an increased amount of electrolyte leakage under saturated humid conditions. Leakage of Potassium hydroxide electrolyte caused damage to the sealant gasket, clogged the oxygen ventilation holes of the batteries, and exhibits high hygroscopic properties when exposed to high temperature and humid conditions.

## KEYWORDS

corrosion, electronics, humidity, KOH electrolyte, zinc air battery

## 1 Introduction

Metal-air batteries have been the most popular source of power for portable electronic devices in the past several decades because of their very high energy densities compared to other battery technologies (Li and Lu, 2017; Aetukuri et al., 2018; Sun et al., 2019). Among the various metal-air technology, zinc-air battery (ZAB) technology seems very promising due to their high volumetric energy density of 1300–1400  $WhL^{-1}$ , safe operation, low

manufacturing cost and environmental friendliness (Sieminski, 2000; Aneke and Wang, 2016; Jing et al., 2016). The ZAB's use oxygen from the surrounding atmosphere to produce electrochemical energy. In general, ZAB's consist of Zn electrode as anode, air electrode as a cathode, porous separator, and alkaline electrolyte, which is usually aqueous potassium hydroxide (KOH) solution. The entire battery assembly is embedded in a metal housing. The zinc electrode and the separator are confined by the housing, while the housing at the air electrode is usually equipped with air holes so that the oxygen, the main reactant at the air electrode, can enter (Reddy, 2011; Schröder, 2016). The air-electrode contains a catalyst that promotes the reaction of oxygen with the electrolyte and the anode Zn-electrode. Gasket-type sealant material is applied on the top battery surface to prevent outgassing and leakage of KOH electrolyte from the battery (Reddy, 2011). Primary aqueous alkaline ZAB are commercially available as small button cells and large cylindrical cells. Nonetheless, ZAB's present several drawbacks, mainly due to the fact that they are half open to the surroundings and can therefore be affected by environmental conditions (Chakkaravarthy et al., 1981; Harting et al., 2012; Chen et al., 2020). The relative humidity, and temperature of the surrounding air can significantly change the interior dynamics of ZAB cells. Alkaline electrolyte such as KOH tends to take up or release humidity from or to the surroundings, depending on the concentration of the electrolyte and its chemical potential. As a result, the performance of ZAB's is strongly affected by changes in climatic conditions during its operation, such that on the dry days, the ZAB might completely dry out and that on humid and hot days, the ZAB might be flooded with water. In both cases, dry out and flooding will lead to ZAB failure, the latter causing leakage of KOH electrolyte due to volume expansion of the cell, pushing the electrolyte out (Balej, 1985; Xu et al., 2013). Further, the water flooding inside the cell can cause corrosion of Zn electrode during battery discharge. The reaction between Zn and  $H_2O$  can lead to the simultaneous production of  $Zn(OH)_2$  and  $H_2$  on the surface of the Zn anode (hydrogen evolution reaction). This corrosion process of Zn anode generated *via* hydrogen evolution reaction can lead to pressure buildup inside the cell, and can cause rupture or break the protective sealant on the battery, causing electrolyte leakage (Faegh et al., 2018).

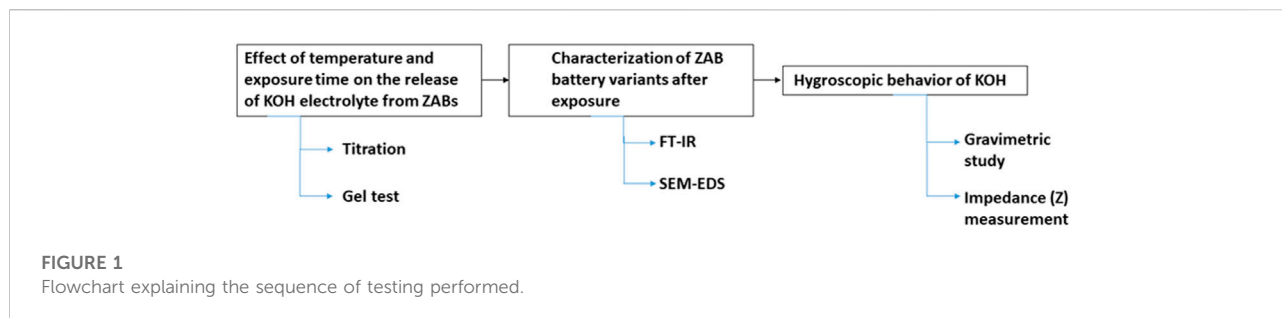
Another factor that is responsible for the leakage of electrolyte from ZAB's is the concentration of dissolved  $CO_2$  in the moisture layer and in the surrounding air. Carbon dioxide from the outer atmosphere can easily be dissolved in the moisture layer, which can enter the battery through the ventilation air holes. It can react with the  $OH^-$  in the electrolyte and decrease its ionic conductivity due to the formation of  $HCO_3^-$  and  $CO_3^{2-}$  and the low solubility of formed  $K_2CO_3$  and  $KHCO_3$  residues. These residues can deposit at the ventilation air holes and can reduce the rate of oxygen diffusion through the air holes, resulting in the performance decline of ZAB. In a situation with high concentration of dissolved  $CO_2$  entering the cell, volume

expansion of the cell, and ultimately leakage of electrolyte (Schröder, 2016; Chen et al., 2020; Hosseini et al., 2021) can occur. Basically, all the reaction kinetics, transport processes, and electrode potential required for the corrosion of Zn anode and for the formation of the organic residues are affected by the temperature inside the cell (Bro and Kang, 1971; Schröder, 2016). Overall, both temperature and relative humidity can influence the ZAB operation and increase the potential for electrolyte leakage.

The leakage of KOH electrolyte from ZAB inside the electronic device when used as a power source can cause severe corrosion failure issues. Major components inside any electronic device include soldering joints, integrated circuits with surface mount components, electrical contacts, *etc.* and are manufactured using materials with good electrical and soldering properties such as Ag, Cu, Al, Sn, Ni, and Au. Several studies in the past have shown the corrosion failures of electrical components in the presence of harsh environmental conditions and ionic contaminants (Waterhouse and Taylor, 1974; Comizzoli et al., 1986; Ohring, 1998; Gudla and Ambat, 2017).

If severe corrosion is evident in the presence of alkaline KOH electrolyte, then the devices that use ZAB's as their primary power source are under severe vulnerability of failure, especially in locations with high temperature and humidity conditions. One such electronic device is hearing aids (HA's) that have been using primary ZAB button cells as their power source since the time of their invention (Jing et al., 2016; Schröder, 2016). Hearing aids are low-power electronic devices that are being used worldwide in a variety of locations that can impose different climatic conditions during its operation e.g., tropical, arid, dry, *etc.* Consequently, HAs are prone to corrosion failures due to moisture layer formation on its electronic parts like print circuit board assembly (PCBA), electrical contacts, *etc.*, under humid conditions as well as upon exposure to bodily fluids such as human sweat and body oils (Gudla and Ambat, 2017). In addition, the failure of ZAB cells in the form of KOH leakage can easily occur with accelerated rates due to the prevalent corrosive environments in which HA devices are operated. Studies conducted on the field failure analysis of hearing aids from different markets revealed that the prominent failure cause for HA devices was the presence of KOH residues from leaking ZAB batteries (Yadav et al., 2021a; Yadav et al., 2021b). All HA electrical components were severely corroded in the presence of KOH electrolyte along with other external residues such as sweat and atmospheric pollutants. The high percentage of failure of HA components due to KOH leakage was observed for tropical regions where the expected conditions of humidity and temperature are always extreme throughout the year, thus increasing the potential for KOH leakage from the batteries.

Although there is literature that has investigated the effect of electrolyte leakage on the performance of ZAB's (Sieminski, 2000; Xu et al., 2013; Schröder, 2016; Faegh et al., 2018), only



limited amount of information is available regarding the synergetic effect of high temperature and humid conditions on the amount of electrolyte release from ZAB's. The study intends to relate the leak of KOH to environmental exposure conditions, as well as the effect on battery deterioration and corrosion issues. The impact of high relative humidity and varying temperature conditions on the amount of electrolyte leakage from ZAB for different exposure times was investigated for three different ZAB variants used widely for HA devices. FTIR analysis was performed to identify the presence of KOH electrolyte on the battery surfaces after their exposure to different climatic conditions. A gel test based on a multiscale pH agar gel indicator was carried out as a qualitative analysis method to visualize the presence of KOH leakage from ZAB, and titration was carried out to quantify the amount of KOH released. The results from these tests were correlated with the *in-situ* voltage discharge of the batteries under varying temperature and humid conditions. Scanning Electron Microscopy (SEM) analysis was performed to characterize the morphology of the released KOH residues and to observe any damage on the battery gasket sealant after their exposure to varying temperature and humidity profile. In addition, the hygroscopicity of KOH residue (laboratory-grade KOH crystals) was evaluated upon its exposure to similar environmental conditions. The hygroscopicity was assessed by a gravimetric study using a water vapor sorption/desorption instrument and by AC electrochemical impedance technique using an interdigitated electrode pattern of a test print circuit board (PCB).

## 2 Materials and methods

Three different manufacturer-based variants of zinc-air batteries typically used for HA application have been selected for investigation in this work, and they are labeled as B1, B2, and B3. These button batteries (size 312) are interchangeable for HA. Batteries B1 and B2 are similar except for the different manufacturers, while battery B3 is meant to be more reliable against humidity and corrosion. Opening in battery B3 for air flow is better protected compared to B1 and B2. Shelf-life for batteries B1 and B2 is approximately 3 years, while for battery

B3 is 5 years. Weight of all batteries are same (0.58 g) as well as the dimensions (height 3.6 mm and diameter 7.9 mm). Voltage and current rating for B1, B2 and B3 are 1.45 V and 160 mAh respectively.

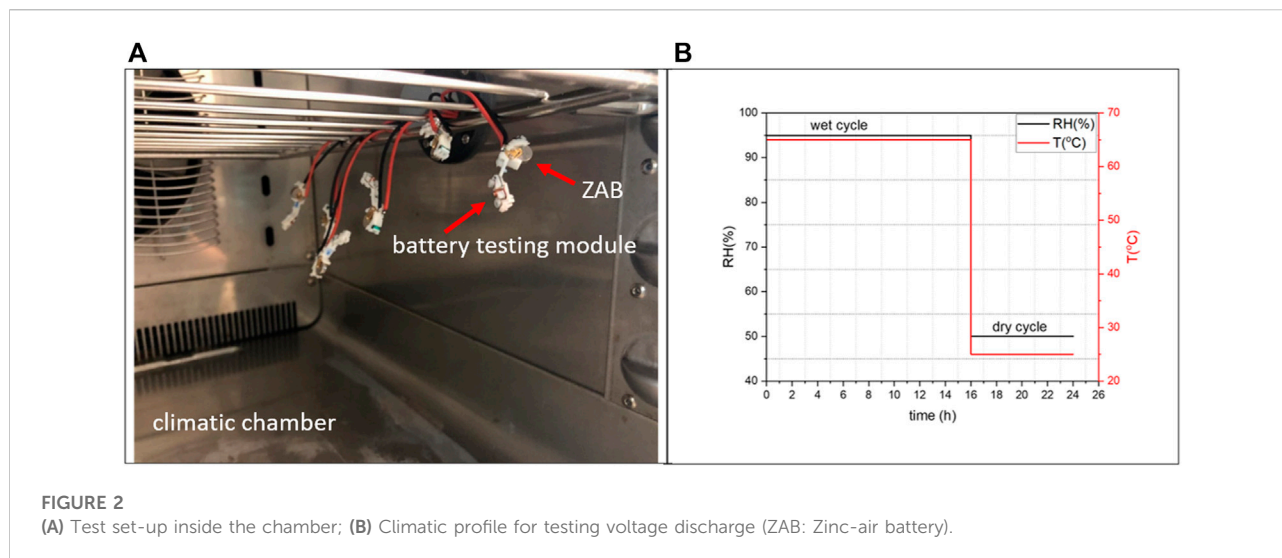
Figure 1 briefly explains various testings done on the battery variants as well as to understand the hygroscopic behavior of KOH using interdigitated test PCBs. These tests were performed at various exposure temperatures of 25°C, 40°C and 60°C. Low to moderate temperatures were chosen (25°C, 40°C) in order to replicate the temperature conditions for various operational regions of HA devices as well as to understand the effect of human body temperature (37°C), while high temperature (60°C) was chosen to accelerate the test conditions.

### 2.1 Effect of temperature and exposure time on the release of KOH electrolyte from ZAB

The battery variants have been analyzed qualitatively (gel test) as well as quantitatively (titration) after different exposure conditions. Qualitative analysis was performed on the batteries to visually confirm the presence of KOH (basic substance) leaked from the batteries when exposed to different conditions of temperature and exposure time. Quantitative analysis was performed to quantify the amount of KOH released from the batteries after the same exposure. A voltage discharge test was also performed for all three battery variants as an attempt to compare their discharge characteristics in dry and humid climatic conditions.

#### 2.1.1 FTIR analysis

FTIR analysis was performed to identify KOH compound on battery surfaces after exposure to humid conditions. The batteries were placed on Petri dishes and 3 ml of deionized water was poured on the samples. The Petri dishes were subsequently covered with a parafilm and left undisturbed at room temperature for 7 days. Subsequently, the Petri dishes were placed in an oven at 40°C to allow crystallization of KOH on the battery surfaces. The chemical analysis was performed on the white residues found on the surface of the batteries. Analytical



grade KOH crystals (analytical purity of 85%–100% supplied by Sigma Aldrich) were analyzed to obtain the reference spectra. As-received batteries were also analyzed for references of a clean surface.

The measurements were conducted at room temperature using ThermoFischer Scientific- Nicolet™ iN™10 MX infrared imaging microscope equipped with a mercury-cadmium-telluride (MCT) detector cooled using liquid nitrogen. The software used for this measurement was OMNIC Picta. The samples were tested using Attenuated Total Reflection (ATR) mode, with a spectral range of  $4000\text{ cm}^{-1}$  to  $675\text{ cm}^{-1}$  (resolution  $4\text{ cm}^{-1}$ ). Characterization of the residue with this technique *via* comparison with the reference spectrum would help confirm the presence of KOH on the battery surfaces, suggesting leakage of the electrolyte.

### 2.1.2 Gel test method (qualitative analysis)

Three batteries of each variant were placed on Petri dishes inside an airtight container with water in it to maintain saturated humid conditions during the test duration. The airtight containers were then exposed to different temperatures at  $25^{\circ}\text{C}$ ,  $40^{\circ}\text{C}$ , and  $60^{\circ}\text{C}$  at exposure times of 1, 5, 7, and 10 days. The objective is to study the synergetic effect of exposure time and temperature on KOH electrolyte release under saturated humid conditions.

At the end of the intended exposure, a multiscale pH indicator in a gel form was applied on the battery surfaces. This indicator has been used on acidic and alkaline compounds prior to the test, which confirmed that a color change from yellow to red/orange indicates the presence of an acidic medium, while a purple coloration indicates an alkaline medium. The visual change in color can help to indicate the leakage of KOH (which is a basic substance) and the associated exposure conditions (exposure time and temperature).

### 2.1.3 Titration test method (quantitative analysis)

Three batteries of each variant were placed on Petri dishes and 3 ml of deionized water was poured on the samples. The Petri dish was subsequently covered with a parafilm and left undisturbed for dedicated exposure conditions. The Petri dishes were exposed to different temperatures:  $25^{\circ}\text{C}$ ,  $40^{\circ}\text{C}$ , and  $60^{\circ}\text{C}$ , for 7 days, to understand the effect of temperature. Similarly, to understand the effect of exposure duration, the batteries were exposed for 1, 5, 7, and 10 days at  $25^{\circ}\text{C}$ .

After the planned exposure, solution (analyte) from the Petri dish potentially containing KOH was extracted using a pipette. 0.01 M HCl solution was used as the titrant, and few drops of phenolphthalein was used as an indicator for titration (for base: phenolphthalein turns the solution pink). The color change from pink to colorless indicated the end-point of titration. The amount of KOH released from the batteries can be estimated by using the equations:

$$C_1 \cdot V_1 = C_2 \cdot V_2 \quad (1)$$

where  $C_1$  is the concentration of HCl (0.01M),  $C_2$  is the concentration of KOH,  $V_1$  is the volume of titrant (HCl), and  $V_2$  is the volume of analyte (KOH).

$$m_2 = C_2 \cdot V_2 \quad (2)$$

where  $m_2$  is the mass of KOH released.

### 2.1.4 Voltage discharge characteristics

The following test was performed to determine the effect of humidity on the voltage discharge characteristics of the three battery variants, in order to correlate and compare the performance degradation of ZAB variants under exposure conditions. Special hearing aid (HA) modules with battery contacts were used to create a circuit to measure the *in-situ* change in their voltage during exposure to dry and wet climatic



**FIGURE 3**  
SIR test PCB used for testing.

cycle for 17 days. Note that no other electronic parts and components of a HA were mounted on the modules. Figure 2A illustrates how an *in-situ* setup with special battery modules held in place inside the climatic chamber was used to conduct the measurements. The voltage discharge tests were performed in climatic chamber Espec SH-641 (fluctuation limits:  $\pm 0.3^\circ\text{C}/3\%\text{RH}$ ).

A multimeter connected to the wires from the modules outside the humidity chamber recorded the DC voltage output of the batteries after every 24 h of cyclic exposure (wet step 95% RH,  $65^\circ\text{C}$  for 16 h followed by a dry step 50% RH,  $25^\circ\text{C}$  for 8 h) (Figure 2B). Similarly, batteries were placed outside the climatic chamber to observe the voltage discharge behavior under room conditions ( $25^\circ\text{C}$ , 40%RH) in order to compare how the storage/shelf life of the batteries varies from those placed inside the climatic chamber.

### 2.1.5 SEM-EDS

The battery variants were characterized to investigate the state of the battery surface and the chemical nature of the corrosion product formed after the batteries were exposed to humid conditions mentioned in Section 2.1.3. This was achieved by using scanning electron microscopy (FEI Quanta 250 AFEG SEM) equipped with energy-dispersive x-ray spectroscopy (EDS) analyzer.

An important part of the batteries failure analysis was to investigate the condition of the sealant gasket. This was important since any damage of the sealant gasket can also result in the leakage of KOH from ZAB's. Another aspect of

the analysis was to observe the condition of the ventilation air holes present in ZAB's. These holes provide a pathway for the entry of oxygen in order to facilitate the reactions inside the batteries. The holes were analyzed to check for the presence of residues that might have leaked from the battery. Furthermore, EDS was performed for the elemental characterization of such residues.

## 2.2 Hygroscopic behavior of KOH

### 2.2.1 Gravimetric test

Water vapor sorption and desorption behavior of KOH was analyzed by gravimetric measurements at constant temperature ( $25^\circ\text{C}$ ) and under humidity range of 10%RH to 90%RH, with a step size of 10% RH. Petri dishes containing KOH crystals (analytical purity of 85%–100% supplied by Sigma Aldrich) were placed inside the equipment. Three repetitions were performed. The default weight limit for measurement was set to +100% of the initial weight, assuming that a further increase in weight would lead to overflow of the deliquesced KOH from the Petri dishes. The sample weight was measured periodically at each RH step using Sartorius Research R 160 P electronic semi microbalance with an accuracy of 0.01 mg.

Saturated moisture content ( $M_{sat}$ ) at each RH level was calculated using the following equation, which is expressed as a percentage of initial weight of the sample:

$$M_{sat} (\text{wt. \%}) = ((m_{sat} - m_d) / m_d) \cdot 100 \quad (3)$$

where  $m_{sat}$  is the mass of the sample at equilibrium, and  $m_d$  is the initial mass of the sample (in dry condition).

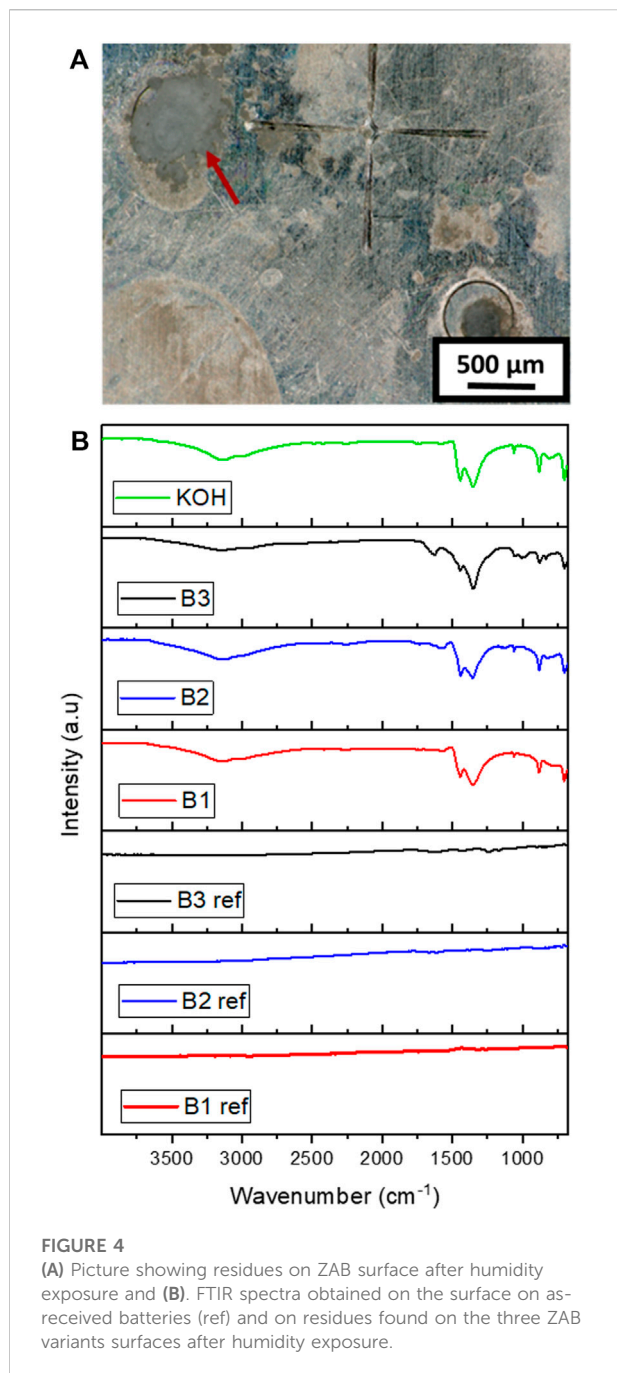
Water sorption and desorption isotherms were generated based on the moisture content in KOH crystals with increasing and decreasing RH levels.

### 2.2.2 Impedance test

Leakage of KOH may contaminate the electronic components present inside the device. Electrochemical impedance spectroscopy enables the monitoring of water film formation due to the presence of the KOH on PCB. The formation of the alkaline media is directly related to a drop in impedance. AC electrochemical measurements were carried out using a test PCB with interdigitated electrode pattern, as shown in Figure 3. The surface finish of the PCB was with hot air solder leveling (HASL). The dimensions of the comb pattern on the SIR test PCBs were  $13 \text{ mm} \times 25 \text{ mm}$  (surface area of  $325 \text{ mm}^2$ ), with a pitch distance of  $300 \mu\text{m}$ .

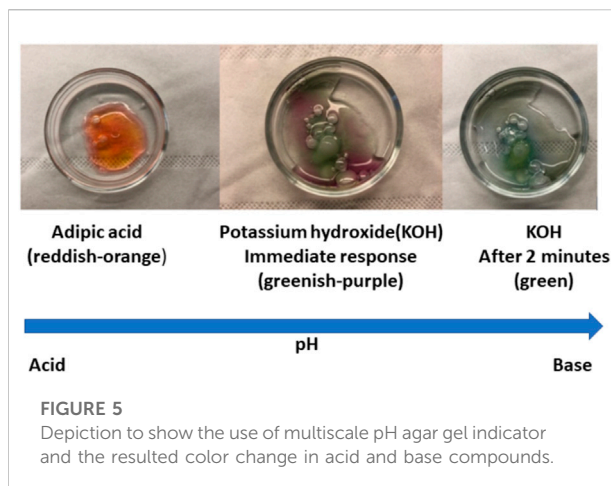
Prior to testing, the SIR test boards were thoroughly rinsed using isopropyl alcohol (analytical purity of 99.8%) and deionized water (conductivity of  $18.2 \text{ M}\Omega \text{ cm}$  at  $25^\circ\text{C}$ ) thrice, followed by drying with pressurized air. A certain volume of a solution of KOH (laboratory-grade KOH crystals from Sigma Aldrich- 85%–100% analytical purity) in isopropyl alcohol was





applied on the comb pattern area in order to achieve a surface concentration of  $100 \mu\text{g cm}^{-2}$ . The samples were left undisturbed at room temperature to allow the solvent to evaporate. The boards were subsequently placed in a desiccator for a day, to remove any volatile compounds that might have been present on it.

The test boards were placed in the climatic chamber (ARL-0680 (fluctuation limits:  $\pm 0.3^\circ\text{C}/2.5\%\text{RH}$ )) at 10%RH and  $25^\circ\text{C}$  for 1 h for the samples and chamber to reach equilibrium. This was



followed by the cyclic climatic profile where RH increased from 10% to 98% for 16 h, followed by a decrease in RH from 98% to 10% for 16 h at  $25^\circ\text{C}$ . Finally, the RH was kept constant at 10% for 16 h to observe the crystallization (efflorescence) behavior of KOH. The impedance measurements were carried out using a “BioLogic VSP” multichannel potentiostat for the entire duration of the test. During the AC measurements, a signal amplitude of 25 mV ( $V_{\text{rms}} = 17.68 \text{ mV}$ ) with a fixed frequency of 10 kHz was applied.

## 3 Results

### 3.1 Effect of temperature and exposure time on the release of KOH electrolyte from ZAB

#### 3.1.1 FTIR analysis of released residues from ZAB

FTIR analysis was performed to characterize the chemical nature of the residues that were found near the ventilation air holes (Figure 4A) in all the three types of ZAB variants (B1, B2, and B3) after their exposure to conditions mentioned in Section 2.1.3. FTIR spectroscopy analysis of these residues was carried out and was compared to the reference spectrum obtained from the surface of fresh battery variants and laboratory-grade KOH crystals. The obtained spectrum from the FTIR analysis is shown in Figure 4B. The spectrum for KOH crystals matches with the spectrum obtained from the residues found on three battery variants, while the spectrum obtained from the fresh batteries did not show any sign of KOH residues. Thus confirming that the residues found on the battery surface is KOH, which is released from the battery upon their exposure to humid climatic conditions.

#### 3.1.2 Gel test method (qualitative analysis)

A multiscale pH indicator mixed with agar gel was used to qualitatively determine the presence of KOH residues on the

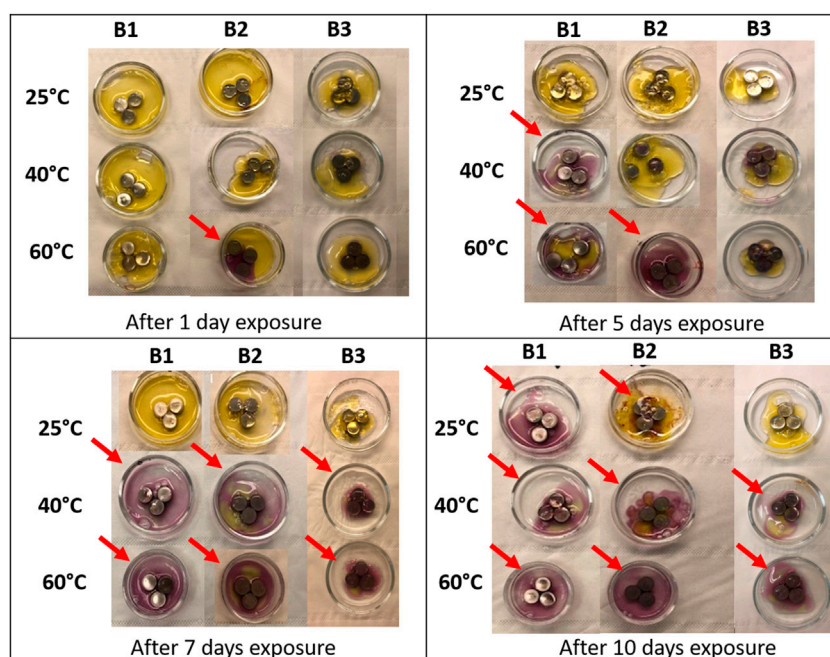


**FIGURE 6**

Application of the multiscale pH gel to the three different ZAB variants after their exposure to different temperatures and varying exposure duration.

battery surfaces after various exposure conditions. The effectiveness of the gel indicator was tested by applying it on dry adipic acid and laboratory-grade KOH crystals to observe any color change. As seen in Figure 5, when the gel indicator was applied to adipic acid, a strong reddish-orange color was observed due to its acidity, while the KOH crystals turned the color from greenish-purple to green due to alkalinity.

Figure 6 shows the application of gel with pH indicator applied on different ZAB variants after their exposure to saturated humidity at different temperatures and varying exposure times. Some batteries showed an immediate color change to purple, indicating the release of KOH. Nevertheless, none of the battery variants showed any sign of KOH leakage from the battery on exposure after 1 day at 25°C and 40°C. The first sign of KOH release from the batteries was observed after 1 day of exposure at 60°C for the B2 variant. Stronger purple color was then observed after 5 days of exposure at 40°C and 60°C for the B1 variant and at 60°C for the B2 variant. Significantly low KOH leakage was observed for the B3 variant at any exposed temperature levels after 5 days. However, all the three battery variants showed significant release of KOH on their exposure to 40°C and 60°C after 7 and 10 days. B1 variant was the only type that showed KOH leakage from the batteries at 25°C after 10 days of exposure time. The tendency of KOH electrolyte leakage from ZAB increases with an increase in temperature and exposure

duration, and B1 battery variant is found to be more susceptible to KOH leakage at low temperature conditions.

### 3.1.3 Titration test method (quantitative analysis)

From another set of experiments, the extracted residues from the ZAB's were titrated against 0.01 M hydrochloric acid to quantify the amount of KOH residues released from the batteries. Figure 7A shows the titration results for the amount of KOH released from three battery variants after immersion in water for different exposure times at 25°C. Results show that there is a significant increase in the amount of KOH leakage for all three battery variants after 7 days of exposure time, with the maximum amount of increase observed for battery variant B2. There is no further increase in KOH leakage observed with an increase of exposure time to 10 days. Repeated experiments in each case showed some variations (as indicated by the error bars) in leakage amount for all the three battery variants, and therefore, only a general observation on their performance is described.

Figure 7B shows the titration result for KOH release after immersion in water at 25°C, 40°C, and 60°C for 7 days. A gradual increase in the amount of KOH released was observed for B2 and B3 with increasing temperature, while a significantly low amount of KOH leakage was observed for B1 variant when compared to the other two variant types. When comparing the two curves (a), and (b) from Figure 7, it is quite evident that temperature has a

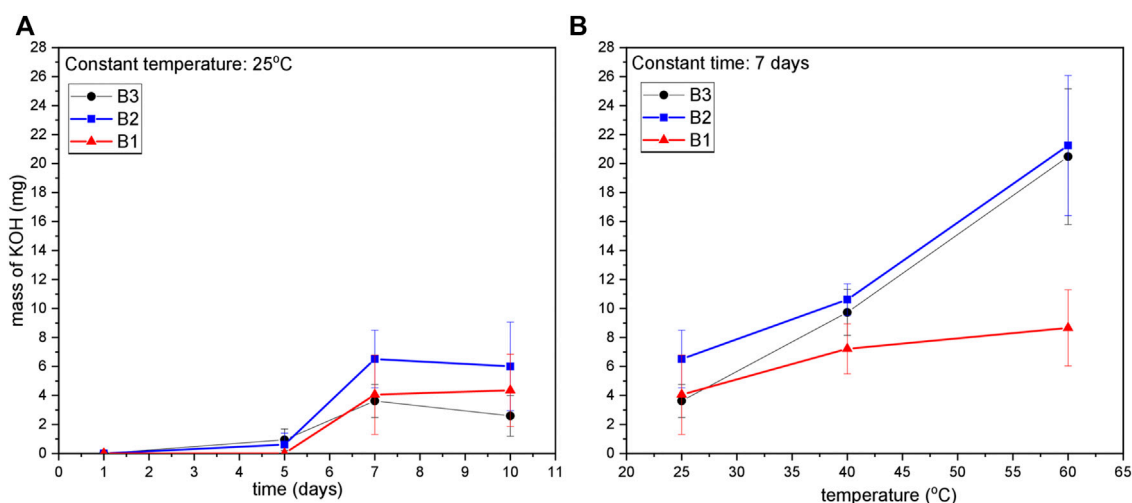


FIGURE 7

Titration result for KOH residue released from three different ZAB variants after their exposure to: (A) Constant temperature of 25°C and varying exposure time, (B) Constant exposure duration of 7 days with varying temperature level.

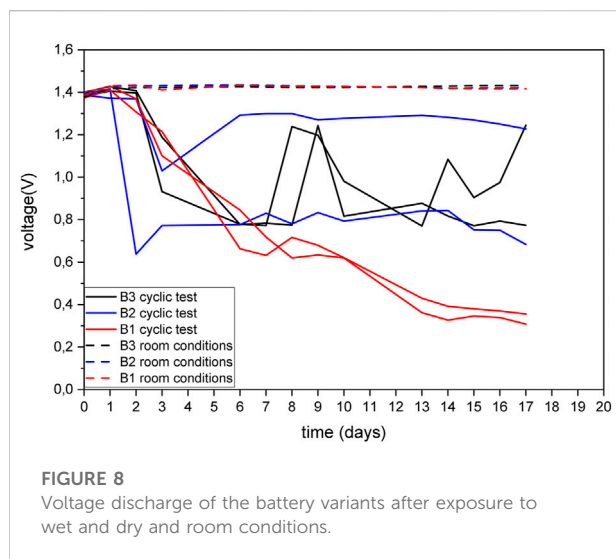


FIGURE 8

Voltage discharge of the battery variants after exposure to wet and dry and room conditions.

greater impact on the amount of KOH released from ZAB's compared to the duration of their exposure to climatic conditions. The variation in the amount of KOH released from ZAB's was found to increase with increasing exposure time and temperature level, with the highest variation was observed after 7 days at 60°.

### 3.1.4 Voltage discharge test

The three variants of the batteries were tested in dry and humid conditions for 17 days following voltage changes. The batteries exposed to the room conditions (25°C and 40% RH) could withstand a constant voltage output during the test, as seen

in Figure 8. Upon exposure to humidity, the voltage discharge readings show a significant amount of fluctuation for the B2 and B3 battery variants. As observed before during the titration analysis, the high variance in KOH electrolyte leakage was found for B2 and B3 variants, which can provide a possible reason for the instability and fluctuation in voltage discharge for the two battery variants. These two battery variants showed a large drop in voltage (up to 0.7 V) just after 3 days of exposure, while there seems to be a gradual decrease in voltage for the B1 variant. Over the duration of the test (about 17 days), the three variants of the batteries showed a decrease in voltage, however they were not fully discharged. B2 and B3 variants showed a lower voltage discharge than B1 (continuous decrease drops up to 0.3 V after 17 days). These results can be correlated to the Gel test, where B1 variant showed higher susceptibility to KOH leakage even at lower temperature conditions.

### 3.1.5 Characterization of ZAB battery variants after their exposure to different temperature and high humidity

Scanning electron microscopy (SEM) analysis was carried out for the three ZAB variants after they were exposed to saturated humidity at 25°C, 40°C, and 60°C for 7 days. Only the effect of temperature is considered for the characterization of the battery variants since it was shown through titration and gel test analysis that 7 days duration leads to high release of KOH from ZAB.

The focus of the analysis here is to observe any structural changes or surface damage that occurred to the battery or the sealant gasket upon their humidity exposure. The surface damage could occur at the ventilation air holes at the back of the battery



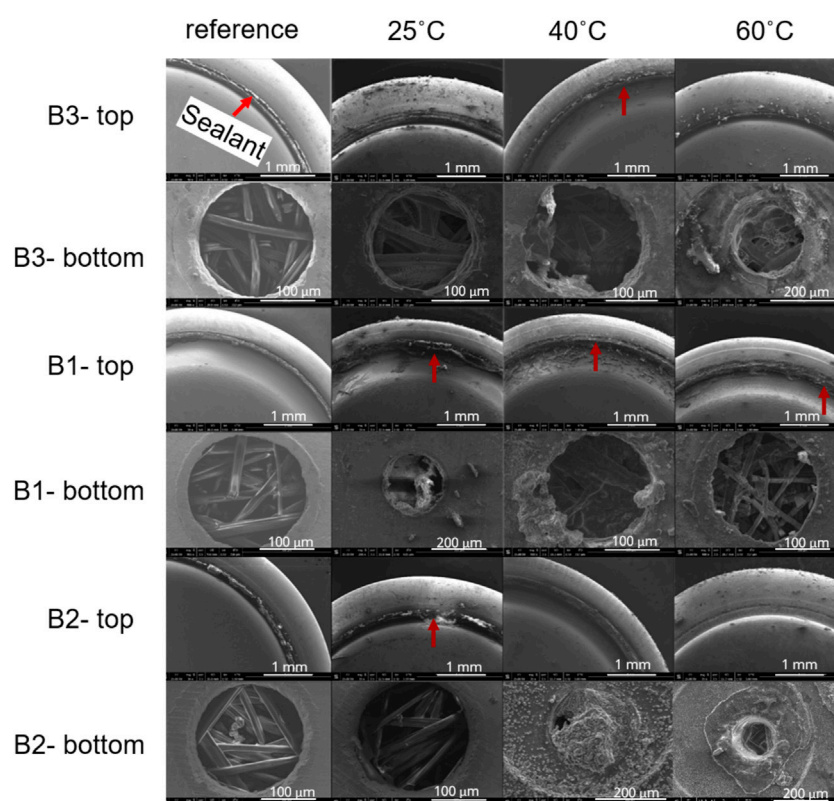


**FIGURE 9**

Secondary electron SEM images of the sealant gasket and the ventilation holes on the ZAB's exposed to different temperatures and constant exposure time of 7 days.

as it is believed to be the primary path for the leakage of KOH electrolyte from the battery.

Figure 9 shows SEM images of the sealant gasket and ventilation air holes for the three ZAB variants when subjected to saturated humidity level at 25°C, 40°C, and 60°C for 7 days. The red arrows shows the structural and morphology changes on the gasket sealant, which might have occurred during the exposure. However, the effect of temperature on the damage of gasket sealant is not very clear since B2 variant showed some kind of structural change or damage to its sealant at 25°C, while no such damage was observed at 40°C, and 60°C. Similarly, battery type B3 showed some structural change or damage on its sealant at 40°C and nothing at 60°C. Notice that the surface of the sealant gasket for all three battery variants were thoroughly investigated under SEM, and only the relevant images are included in this study.

It is indeed important to know if the damage found on the gasket sealant is big enough to allow any leakage of KOH electrolyte from the battery. Therefore, to get a better overview of the elemental composition of the residues and understand the extent of damage to the sealant gasket, EDS elemental mapping (Figure 10A) was carried out on one of the

battery variant (B2 at 25°C), where some structural changes due to damage (Figure 9) to the sealant gasket was observed.

The EDS elemental maps of the gasket sealant shows the presence of F, K, O, and Zn elements. The other elements from the battery material are not shown in the analysis. The distribution of K map follows the distribution of O, suggesting the possibility of KOH presence. The presence of KOH residues in the vicinity of the sealant was identified and thus confirming the damage that occurred to the sealant gasket. The presence of Zn could possibly be because of the corrosion of Zn electrode in the presence of water and subsequent generation of hydrogen gas. The corrosion products of Zn are pushed outside the battery along with KOH electrolyte due to cell volume expansion. Some part of O map follows the distribution of Zn, thereby possibly indicating the presence of Zn-O based corrosion products. F element comes from the material composition of gasket sealant. It is possible that the KOH residues are moved to the sealant gasket area upon its release from the ventilation holes present at the backside. However, the EDS mapping showed that the characteristics X-rays of K, O and Zn elements are more pronounced at the damaged sealant gasket surface, than other areas near the gasket.

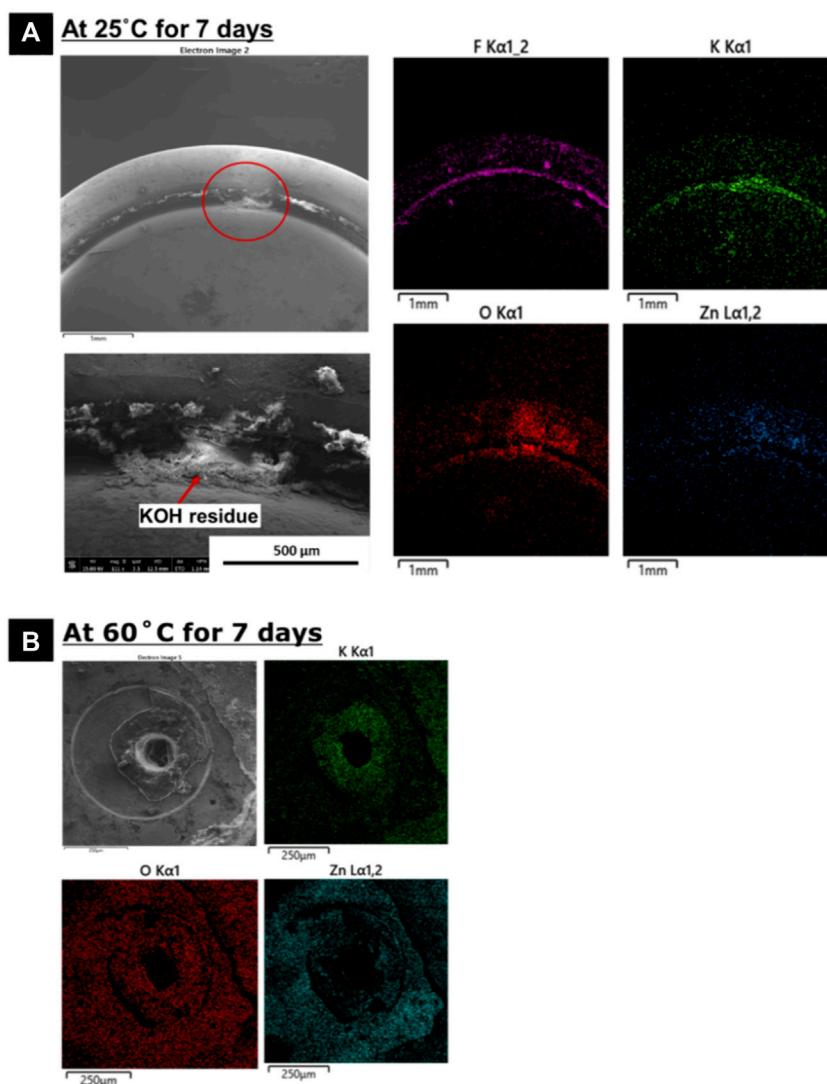


FIGURE 10

Secondary electron images and EDS elemental maps for B2 variant after exposure: (A) Sealant gasket, (B) Residues found on ventilation holes.

The ventilation air holes shows the presence of residues in and around it for all the three battery variants (Figure 9). The amount of residues seems to be greater in amount for batteries exposed to higher temperatures namely 40°C, and 60°C. The residues also seem to have clogged the entire ventilation hole for B2 variant exposed to 40°C and 60°C, while a similar observation was made for B3 variant when exposed to 60°C. High amount of KOH residue are observed at the air holes for B2 variant compared to the other two variant type. EDS elemental mapping was done in order to get a better overview of the elemental composition of these residues at air holes. The EDS elemental maps (Figure 10B) shows that it consists of K, Zn, and O. The distribution of Zn and K follows the distribution of O,

suggesting the presence of possible KOH residue along with Zn-O based corrosion products.

## 3.2 Hygroscopic behavior of KOH

### 3.2.1 Gravimetric study of KOH

The sorption and desorption behavior of KOH crystals is presented in Figure 11 showing the saturated amount of water vapor absorbed as a function of RH level at a constant temperature of 25°C. The moisture sorption cycle was manually stopped when 50% RH was reached, before the equilibrium state of water sorption. This was done to prevent

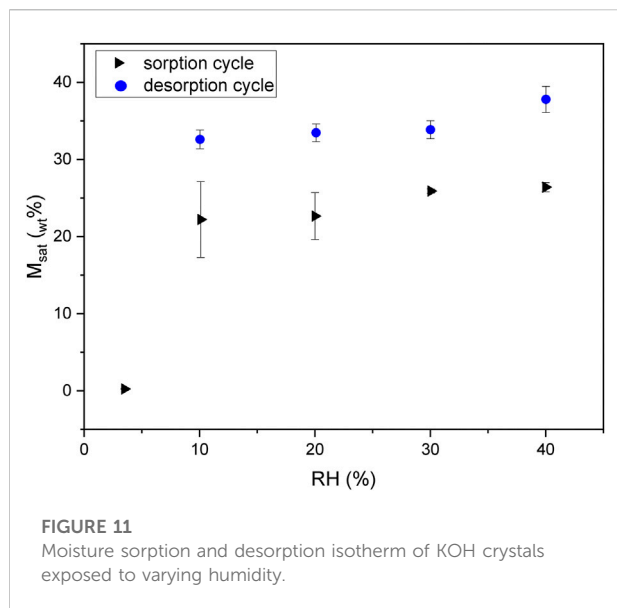


**FIGURE 11**  
Moisture sorption and desorption isotherm of KOH crystals exposed to varying humidity.

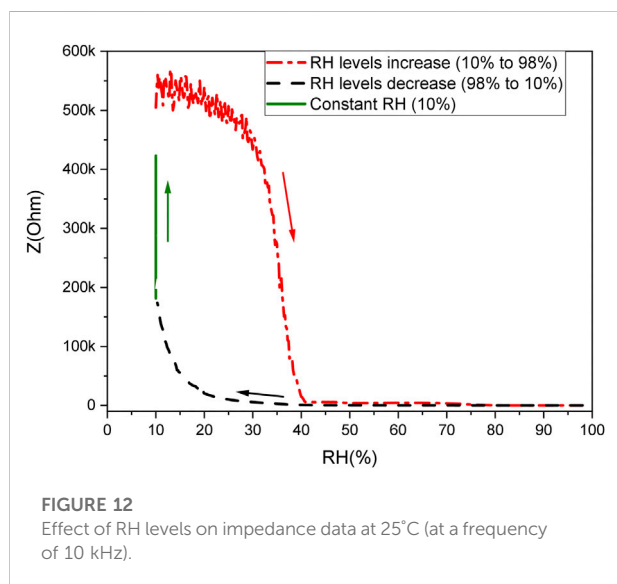


**FIGURE 12**  
Effect of RH levels on impedance data at 25°C (at a frequency of 10 kHz).

the damage of the measuring equipment due to the overflow of deliquesced KOH. Afterward, the RH was decreased from 50% to 10% to study the moisture desorption behavior of KOH crystals.

The KOH crystals shows early water uptake at the lowest RH of 10% within some hours of starting the test, reaching about 20<sub>wt</sub>% of mass gain (water absorption). The saturated weight gain ( $M_{sat}$ ) for KOH increases at a slower rate on increasing the RH from 10% to 40%, with an up to ~25<sub>wt</sub>% measured at the end of 40% RH step. When the climate set up reached 50% RH, a sudden onset of KOH crystals deliquescence was observed, with a sharp and significant increase in the amount of water vapor absorbed by KOH crystals, which was found to be increasing at a

steep rate until the test was stopped manually, before the equilibrium was reached (therefore  $M_{sat}$  is not shown in Figure 11).

The desorption curve proceeds with decreasing the RH from 50% to 10%, where deliquescent KOH crystals starts to show a decrease in mass gain due to the release of absorbed water molecules at the step of 30% RH. However, on decreasing the RH, the KOH crystals did not completely crystallize, and therefore, the desorption curve lies above the sorption curve. Even after keeping the RH constant at 10% for a day, the KOH residues did not allow complete desorption of water molecules.

### 3.2.2 Impedance test using KOH contaminated PCB

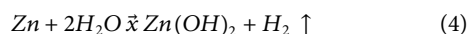
The test was carried out on interdigitated test PCB pre-contaminated with 100  $\mu\text{g cm}^{-2}$  of KOH and exposed to 25°C, subjected to increase and decrease of RH levels (10–98% RH). AC test (Figure 12) was performed along with three steps of 16 h, namely during 1) RH levels increase (10%–98%), 2) RH levels decrease (98%–10%), and 3) constant RH (10%). During the slow increase of RH level, a sudden drop of impedance is observed at around 30% RH and remained low up to 98% RH. This confirms that KOH starts absorbing water at very low level of RH, and that a water layer starts building up on the PCB surface when exposed to 30% RH, and remained present (related to drop of impedance). During the gradual decrease of RH from 98% to 10%, the impedance remained low and started only to increase again when 30% RH was reached but did not retrieve its initial value. The test PCB was then exposed to a constant RH level of 10% for 16 h. The impedance continued to increase but did not reach the initial impedance value. This indicates that a thin water film is still present on the PCB surface, and did not dry out upon the long exposure to dry conditions, maintaining a critical condition (presence of electrolyte on PCB surface), that can lead to electronic malfunction and corrosion issues.

## 4 Discussion

The Gel test and Titration test showed the occurrence of KOH leakage from the three different ZAB variants when exposed to different temperatures and exposure time. High variance in the leakage of KOH residues was observed for both qualitative and quantitative analysis, and therefore a clear correlation between various factors causing the battery leakage is difficult to make. Thus, on analyzing the results from both the tests in a broader sense, it can be inferred that high temperature conditions have a more pronounced effect on the amount of KOH leakage from ZAB under saturated humid conditions as compared to the duration of exposure. However, it can be noted that B3 variant, meant to be used in high humidity conditions, did not show improved reliability towards humidity compared to B1 and B2.

The battery analysis after their exposure to different temperatures and under saturated humidity showed the presence of a high amount of KOH residues and Zn-O-based corrosion products around the ventilation holes. Similar chemical compounds were found on the sealant gasket of the batteries, and therefore it becomes important to discuss in depth the process of Zn electrode corrosion and its effect in causing leakage of KOH electrolyte from the ZAB.

The active anode Zn material of the ZAB undergoes an oxidation process during the cell discharge and involves several other processes such as dissolution of ions in the solution, ion diffusion in the electrolyte, and precipitation into a solid phase when the solubility limit is reached (Caramia and Bozzini, 2014). However, in conditions when water is present inside the battery, the corrosion of Zn electrode can take place in an aqueous KOH electrolyte to produce hydrogen gas according to reaction 4.



Corrosion of Zn in the presence of water and KOH electrolyte will produce a black deposit and hydrogen evolution, which is known to cause cell rupture, damage of the sealant gasket, and leakage of electrolyte (Caramia and Bozzini, 2014; Faegh et al., 2018). Also, it is worth mentioning that under alkaline pH electrolyte (pH < 13), more stable type II ZnO is formed due to the passivation of Zn, which can hinder the further dissolution of Zn, and can make the anode surface electrochemically inactive, thus making the battery inconvenient to operate (Thomas et al., 2013).

The voltage discharge test showed high fluctuation in voltage readings of B2 and B3 battery variants, whereas a gradual decrease of voltages was observed for B1. This fluctuation in the voltage during discharge can be attributed to the lowering of KOH electrolyte molarity due to the ingress of water vapor inside the cell and diluting the electrolyte, thus affecting its performance (Schröder, 2016). Furthermore, the release of KOH and the production of carbonate products during humidity and temperature exposure can clog the ventilation holes of the battery, which can decrease the availability of oxygen at the air electrode, thus causing performance degradation of the batteries.

The water absorption test showed that KOH is highly hygroscopic (Figure 11) and starts absorbing moisture at RH level as low as 10% (about 20 wt%). This was correlated with the EIS test (Figure 12), where the impedance starts to drop at low RH levels, with a subsequent sudden drop at around 30% RH. During the drying cycle, a hysteresis can be observed, and even after a constant exposure at 10% RH for 16 h, low impedance levels indicate the presence of a remaining water layer on the surface of the test PCB. The hygroscopic nature of the residues was clearly depicted in this test and therefore, the leakage of KOH electrolyte inside an electronic device can lower the RH boundary for the device through the process of deliquescence and will therefore cause thick water layer formation. Variety of electronics

failure modes due to humidity has been reported previously, of which the thickness of water layer formed on the electronic components like PCBA is the most critical factor determining the reliability of electronics (Piotrowska et al., 2015; Conseil-Gudla et al., 2017; Ambat et al., 2018). This is significantly affected by the presence of ionic contamination on the PCBA surface and their hygroscopicity.

Our previous work on the failure analysis of field failed hearing aids from various markets revealed that KOH electrolyte leakage from the ZAB power source was the major failure cause (Yadav et al., 2021a; Yadav et al., 2021b). The failure percentage of devices due to KOH was higher for tropical regions. The KOH residues caused degradation of conformal coatings on PCBA and other hand soldering areas, which subsequently caused severe localized corrosion attacks. Due to their high solubility, the KOH residues were able to easily dissolve in the moisture and human sweat formed inside the device upon exposure to the human body and harsh climatic conditions of tropical regions. As a result, they ionized on dissolving into the liquid to form  $\text{OH}^-$  ions, which traveled to various components of the HA device and in particular, affected the components having high electric potential. For example, the microphone component of HA, due to the presence of a high electrical charge on its membrane plate, was able to preferentially attract hydroxide ions of KOH. This led to heavy corrosion of the adjacent electrical components such as capacitors and resistors, up to their complete failures. Hence, the presence of these hygroscopic KOH residues on the surface of electronic boards and components can be detrimental to electronics reliability due to their ease of absorbing moisture at lower RH levels.

The critical RH (cRH) for hygroscopic substance, also defined as the deliquescence point, is when the phase transformation occurs from a solid to a saturated solution at a particular RH level. Above this cRH level, there exists a chemical potential between the water on the surface of the crystal and the water present in the air. This gradient acts as a driving force for water condensation to take place on the crystal and gradually leads to the dissolution of the crystals if the conditions are maintained above cRH (Piotrowska et al., 2018). Thus, the presence of an aggressive environment (elevated temperature and high humidity), along with the presence of KOH, provides a suitable condition for the formation of a corrosion cell and leads to the reduction of surface insulation resistance (SIR) between electrical conductors (Piotrowska et al., 2017), parasitic leak current and intermittent failures, up to device failures (Sinclair, 1988; Verdingovas et al., 2015).

Several studies have reported previously that the solder flux residues that remain on the surface of the PCBA surface after the soldering process can lower the corrosion reliability of the device in humid environment (Zhan et al., 2008; Verdingovas et al., 2015; Piotrowska et al., 2018). These residues showed high hygroscopic behavior and solubility in water, which resulted in their high susceptibility to form an electrolyte with high



conductivity, and showed increase leak current and ECM failures (Sohn and Ray, 1995; Zou and Hunt, 1999). Deliquescence relative humidity (DRH) reported in previous studies for flux activators, and salt residues showed that compared to flux activators, salt residues have low RH for deliquescence, with Cl salts of Mg and Ca showed the lowest RH for deliquescence at 44% and 29% RH, respectively. Similarly, in comparison, the presence of alkaline KOH residues inside an electronic device should exhibit similar RH for deliquescence like salt residues, which can accelerate the corrosion of electronic board assembly and its components.

## 5 Conclusion

The present study showed that the climatic exposure related degradation of ZAB and electronic parts due to KOH release should be taken in consideration.

- 1) The Gel and Titration test revealed the release of KOH electrolyte from the three ZAB variants, particularly at high temperatures and saturated humid conditions, and was found to increase with increasing exposure duration. Among the two effects, the temperature has a higher impact on the leakage of KOH than exposure duration under saturated humid conditions. High variance in the amount of KOH leakage from ZAB was observed for B2 and B3 and was correlated with the fluctuation in voltage drop observed during the voltage discharge test. B1 showed higher susceptibility towards KOH leakage from ZAB upon exposure to different temperature conditions.
- 2) SEM-EDS analysis of the battery surface after their exposure to different temperatures under saturated humidity showed Zn-O-based corrosion products along with KOH residues. Outgassing caused by the release of hydrogen gas during the corrosion of Zn electrode was linked to the damage found on the battery sealant gasket.
- 3) KOH residues were found to be highly hygroscopic in nature and start absorbing water from the surrounding air at very low RH levels ( $\sim 20$  wt% at 10% RH). Similar hygroscopic behavior of KOH residues was observed during EIS testing. This hygroscopic behavior of KOH can lead to the formation of a sufficient amount of water on electronics PCBA surface with high conductivity, thus causing a huge drop in

impedance and increases the risk of other corrosion failure modes.

## Data availability statement

The original contributions presented in the study are included in the article/Supplementary Material, further inquiries can be directed to the corresponding author.

## Author contributions

JR, experimental and data analysis, writing—review and editing. AY, investigation, supervision, original draft. HC-G, investigation, supervision, writing—review and editing. RA, project leader, supervision, writing—review and editing.

## Acknowledgments

This research reported here was conducted as a part of the Industrial PhD project, and the authors would like to acknowledge the funding and help received from Innovation Fund Denmark.

## Conflict of interest

AY was employed by WS Audiology.

The remaining authors declare that the research was conducted in the absence of any commercial or financial relationships that could be construed as a potential conflict of interest.

## Publisher's note

All claims expressed in this article are solely those of the authors and do not necessarily represent those of their affiliated organizations, or those of the publisher, the editors and the reviewers. Any product that may be evaluated in this article, or claim that may be made by its manufacturer, is not guaranteed or endorsed by the publisher.

## References

- Aetukuri, N. B., Jones, G. O., Thompson, L. E., Ozgit-Akgun, C., Akca, E., Demirci, G., et al. (2018). Ion pairing limits crystal growth in metal-oxygen batteries. *ACS Energy Lett.* 3, 2342–2348. doi:10.1021/acsenergylett.8b01387
- Ambat, R., Conseil-Gudla, H., and Verdingovas, V. (2018). Corrosion in electronics. *Encycl. Interfacial Chem. Surf. Sci. Electrochem.* 9, 134–144. doi:10.1016/B978-0-12-409547-2.13437-7
- Aneke, M., and Wang, M. (2016). Energy storage technologies and real life applications – a state of the art review. *Appl. Energy* 179, 350–377. doi:10.1016/j.apenergy.2016.06.097
- Balej, J. (1985). Water vapour partial pressures and water activities in potassium and sodium hydroxide solutions over wide concentration and temperature ranges. *Int. J. Hydrogen Energy* 10, 233–243. doi:10.1016/0360-3199(85)90093-X

- Bro, P., and Kang, H. Y. (1971). The low-temperature activity of water in concentrated KOH solutions. *J. Electrochem. Soc.* 118, 1430. doi:10.1149/1.2408345
- Caramia, V., and Bozzini, B. (2014). Materials science aspects of zinc-air batteries: A review. *Mat. Renew. sustain. Energy* 3, 28. doi:10.1007/s40243-014-0028-3
- Chakkaravarthy, C., Waheed, A. K. A., and Udupa, H. V. K. (1981). Zinc-air alkaline batteries - a review. *J. Power Sources* 6, 203–228. doi:10.1016/0378-7753(81)80027-4
- Chen, P., Zhang, K., Tang, D., Liu, W., Meng, F., Huang, Q., et al. (2020). Recent progress in electrolytes for Zn-air batteries. *Front. Chem.* 8, 372. doi:10.3389/fchem.2020.00372
- Comizzoli, R. B., Frankenthal, R. P., Milner, P. C., and Sinclair, J. D. (1986). Corrosion of electronic materials and devices. *Science* 80, 340–345. doi:10.1126/science.234.4774.340
- Conseil-Gudla, H., Jellesen, M. S., and Ambat, R. (2017). Printed circuit board surface finish and effects of chloride contamination, electric field, and humidity on corrosion reliability. *J. Electron. Mat.* 46, 817–825. doi:10.1007/s11664-016-4974-7
- Faegh, E., Omasta, T., Hull, M., Ferrin, S., Shrestha, S., Lechman, J., et al. (2018). Understanding the dynamics of primary Zn-MnO<sub>2</sub> alkaline battery gassing with operando visualization and pressure cells. *J. Electrochem. Soc.* 165, A2528–A2535. doi:10.1149/2.0321811jes
- Gudla, V. C., and Ambat, R. (2017). Corrosion failure analysis of hearing aid battery-spring contacts. *Eng. Fail. Anal.* 79, 980–987. doi:10.1016/j.engfailanal.2017.05.045
- Harting, K., Kunz, U., and Turek, T. (2012). Zinc-air batteries: Prospects and challenges for future improvement. *Z. Fur Phys. Chem.* 226, 151–166. doi:10.1524/zpch.2012.0152
- Hosseini, S., Masoudi Soltani, S., and Li, Y. Y. (2021). Current status and technical challenges of electrolytes in zinc-air batteries: An in-depth review. *Chem. Eng. J.* 408, 127241. doi:10.1016/j.cej.2020.127241
- Jing, F., Paul, C. Z., Gyu, P. M., Aiping, Y., Michael, F., and Zhongwei, C. (2016). Electrically rechargeable zinc-air batteries: Progress, challenges, and perspectives. *Adv. Mat.* 29, 1604685. doi:10.1002/adma.201604685
- Li, Y., and Lu, J. (2017). Metal-air batteries: Will they Be the future electrochemical energy storage device of choice? *ACS Energy Lett.* 2, 1370–1377. doi:10.1021/acsenergylett.7b00119
- Ohring, M. (1998). Degradation of contacts and package interconnections. *Reliab. Fail. Electron. Mat. Devices* 79, 475–537. doi:10.1016/b978-012524985-0/50010-6
- Piotrowska, K., Jellesen, M. S., and Ambat, R. (2017). Thermal decomposition of solder flux activators under simulated wave soldering conditions. *Solder. Surf. Mt. Technol.* 29, 133–143. doi:10.1108/SSMT-01-2017-0003
- Piotrowska, K., Ud Din, R., Grumsen, F. B., Jellesen, M. S., and Ambat, R. (2018). Parametric study of solder flux hygroscopicity: Impact of weak organic acids on water layer formation and corrosion of electronics. *J. Electron. Mat.* 47, 4190–4207. doi:10.1007/s11664-018-6311-9
- Piotrowska, K., Verdingovas, V., Jellesen, M. S., and Ambat, R. (2015). "Contamination, potential bias and humidity effects on electrical performance and corrosion reliability of electronic devices," in *Eur. Corros. Congr. EUROCORR* (Graz, Austria: EUROCORR).
- Reddy, T. B. (2011). *Button cell batteries: Silver oxide-zinc and zinc-air systems*. New York: McGraw-Hill Education. AvailableAt: <https://www.accessengineeringlibrary.com/content/book/9780071624213/chapter/chapter13>.
- Schröder, D. (2016). *Analysis of reaction and transport processes in zinc air batteries*. Wiesbaden: Springer.
- Sieminski, D. (2000). "Primary zinc-air for portable electronic consumer products," in *Proc. Annu. Batter. Conf. Appl. Adv.*, Long Beach, CA, USA, 12–15 January 1999 (IEEE). doi:10.1109/BCAA.2000.838390
- Sinclair, J. D. (1988). Corrosion of electronics: The role of ionic substances. *J. Electrochem. Soc.* 135, 89C–95C. doi:10.1149/1.2095755
- Sohn, J. E., and Ray, U. (1995). Weak organic acids and surface insulation resistance. *Circuit World* 21, 22–26. doi:10.1108/eb044046
- Sun, Y., Liu, X., Jiang, Y., Li, J., Ding, J., Hu, W., et al. (2019). Recent advances and challenges in divalent and multivalent metal electrodes for metal-air batteries. *J. Mat. Chem. A Mat.* 7, 18183–18208. doi:10.1039/c9ta05094a
- Thomas, S., Birbilis, N., Venkatraman, M. S., and Cole, I. S. (2013). Self-repairing oxides to protect zinc: Review, discussion and prospects. *Corros. Sci.* 69, 11–22. doi:10.1016/j.corsci.2013.01.011
- Verdingovas, V., Jellesen, M. S., and Ambat, R. (2015). Solder flux residues and humidity-related failures in electronics: Relative effects of weak organic acids used in No-clean flux systems. *J. Electron. Mat.* 44, 1116–1127. doi:10.1007/s11664-014-3609-0
- Waterhouse, R. B., and Taylor, D. E. (1974). Fretting debris and the delamination theory of wear. *Wear* 29, 337–344. doi:10.1016/0043-1648(74)90019-2
- Xu, Y., Xu, X., Li, G., Zhang, Z., Hu, G., and Zheng, Y. (2013). Experimental research of liquid infiltration and leakage in zinc air battery. *Int. J. Electrochem. Sci.* 8 (10), 11805–11813.
- Yadav, A., Kumar Gupta, K., Ambat, R., and Espersen, C. (2021). A comparative study on corrosion failure analysis of hearing aid devices from different markets. *Microelectron. Reliab.* 1–15. doi:10.1002/maco.202213420
- Yadav, A., Kumar Gupta, K., Ambat, R., and Løgstrup Christensen, M. (2021). Statistical analysis of corrosion failure of hearing aid devices used in tropical regions. *Eng. Fail. Anal.* 130, 105758. doi:10.1016/j.engfailanal.2021.105758
- Zhan, S., Azarian, M. H., and Pecht, M. (2008). Reliability of printed circuit boards processed using no-clean flux technology in temperature-humidity-bias conditions. *IEEE Trans. Device Mat. Reliab.* 8, 426–434. doi:10.1109/TDMR.2008.922908
- Zou, L., and Hunt, C. (1999). Surface insulation resistance (SIR) response to various processing parameters. *Solder. Surf. Mt. Technol.* 11, 30–34. doi:10.1108/09540919910265668